A COMPARATIVE ANALYSIS OF LOWER SPEED CHATTER BEHAVIOUR

Pavel Bach[1], Milos Polacek[1], Petr Chvojka[1], Jiri Drobilek[1]
Ondrej Svoboda[2]
[1]CTU in Prague, Research Center of Manufacturing Technology
Prague, Czech Republic
[2]Misan, s. r. o., Lysa nad Labem, Czech Republic
e-mail: info@rcmt.cvut.cz, lysa@misan.cz

It is known that reduced cutting speeds increase the limit of stability. However, this only applies to milling operations. In turning operations the stability limit initially drops with decreased cutting speed and subsequently rises with a further decrease in cutting speed. A minimum of attention is devoted to this phenomenon in the literature although many authors have noted the decline in the limits of stability during machining tests. In practice, it is important to know the conditions and extent of this decline. This paper summarizes previously published data and provides new data, measured by the authors of the paper. A comparison of the conditions used in the turning tests shows that the decline in the limits of stability and its subsequent increase in the area of lower cutting speed only occur when using a tool with a small clearance angle. A new analysis of the previously published data from the measurement of dynamic cutting force coefficients revealed that the drop in the stability is affected by changing the mutual phase of the dynamic cutting forces and tool vibration.

Keywords
chatter stability drop, turning, lower speed

1. Introduction

A sufficiently accurate stability diagram continues to be a high priority in research in the field of cutting dynamics. The knowledge of the stability diagram is essential not only in order to achieve higher rough milling performance, utilizing its gaps among lobes for a choice of higher depth of cut, but also in order to identify a chatter free spindle speed for finishing operations, for which machined surface quality achieved in minimum productive time is the criterion of success. The stability diagram should also predict cutting conditions at lower cutting speeds used for machining difficult-to-cut materials and where process damping occurs.

The characteristic of the stability limit in the lower cutting speed region may differ for turning and milling operations (see Fig. 1). While in milling the stability limit rises with decreasing cutting speed, in turning the stability limit first drops and subsequently rises if the cutting speed is decreased. In both cases, with the exception of the mentioned drop, the stability limit is considerably higher at the lowest cutting speeds used than at common or high cutting speeds. Both curves shown are in fact envelopes of overlapping lobes, which merge in the area of lower cutting speeds.

In this paper, the authors would like to a) find some technological conditions under which the undesirable turning stability drop occurs, and b) contribute to the explanation of the mechanism of the stability drop.

To simplify and shorten the explanation in proper cases, we will call the hyperbolic-shaped stability limit curve the L-curve and the bowl-shaped curve the U-curve.

2. Examples of cutting (turning) test results

There is a great deal of evidence in the literature for the difference in stability limit curves for turning and milling. Authors agree that the rise in stability is caused by the effect of process damping, i.e. by the influence of damping forces from the cutting process, not on the machine tool frame. Although some joint research of several laboratories, commented in [Peters 1972] and analysed in [Tlusty 1978] highlighted the drop in the stability limit while turning, it seems that no one has so far investigated either the physical causes of this phenomenon or the difference in the characteristic of the stability limit in turning and milling. There is one exception, the investigators Liu C. R., and Liu T. M. [Liu 1985], who suggested chatter suppression by means of changeable geometry of the tool while turning. They observed the different form of the stability curves when the tool geometry was changed. Below we will present several examples of machining test results by different authors and from different time periods, and we will compare stability limit curves for turning and milling.

Sisson [Sisson 1969] present stability limit measurements for orthogonal turning of the titanium alloy B120VCA. Although it was difficult to keep the condition of the cutting tool edge constant during machining, there were no significant deviations in the measured data. This is evidenced by the stability limit graph in Fig. 2. Points delineating both the unstable area (chatter) and stable area suggest a drop in stability with a minimum around the speed 40 m/min.

Kals [Kals 1971] measured the stability limit under conditions of orthogonal turning. The workpiece material was AISI1045 normalized and the cutting tool had the following parameters: rake angle 5°, clearance angle 6°, approach angle 90°, tool nose radius 0.4 mm, feed rate 0.072 mm/rev. For their results refer to Fig. 3.

At a CIRP meeting in 1972, Peters et al. [Peters 1972] reported the methods and results of a collaborative project on measuring dynamic cutting force coefficients (DCFC), and presented, apart from other things, the graphs in Fig. 3.

The project participants included the research laboratories of Leuven, Eindhoven, Birmingham and Aachen University and the Research

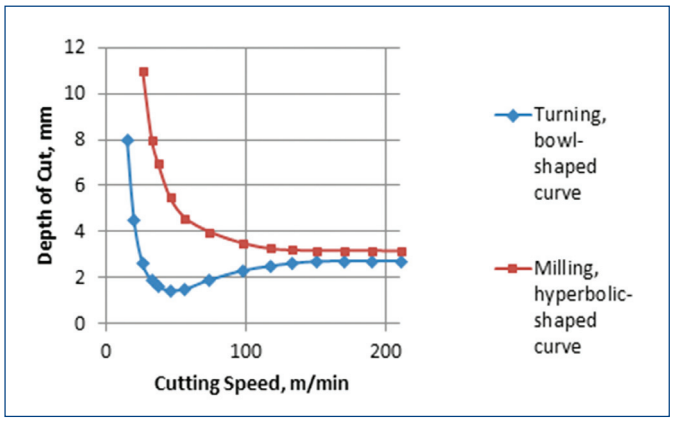

Figure 1. *Different characteristic of stability limit curves for turning and milling.*

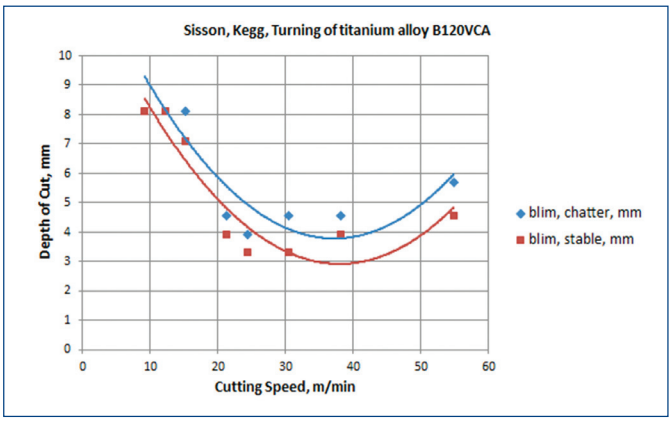

Figure 2. *Stability of orthogonal turning of Ti-alloy B120VCA after [Sisson 1969].*

Institute for Machine Tools and Machining in Prague (VÚOSO). The result measured in Aachen is presented separately in Fig. 5 together with other similar curves. The values of the stability limit from Eindhoven, Birmingham and Prague had practically the same characteristic. They differed in tens of millimeters and are averaged under the label "CIRP average". The values measured in Leuven were approximately 1.5 mm higher and are plotted separately. All curves had a minimum around 80 m/min. There is no indication that the curves level off above 100 m/min within the cutting speed range used. Nevertheless, it can be said that process damping does not dominate in the whole measured extent of speeds, but only up to 80 m/min. The drop in the stability is significant.

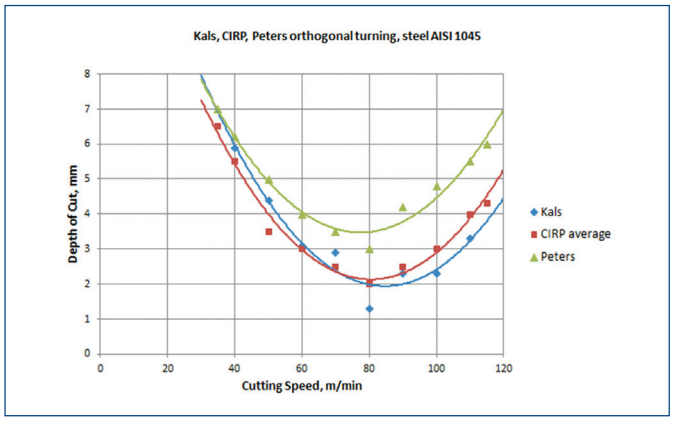

Figure 3. *Stability of orthogonal turning for steel AISI1045 (C45), data compiled after [Kals 1971] and [Peters 1972].*

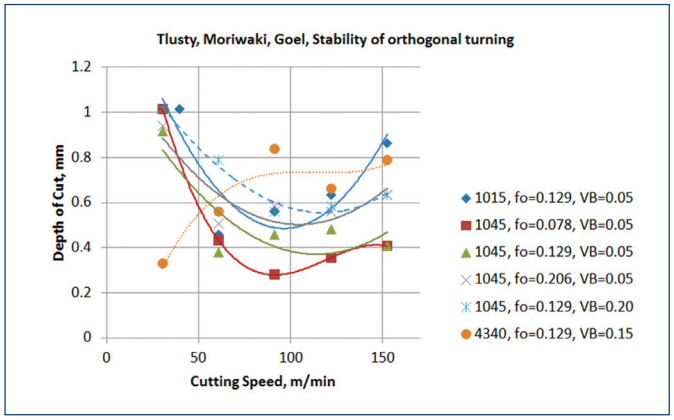

Figure 4. *Influence of feed rate and tool wear in stability. Data compiled after [Tlusty 1976].*

The measurement from Aachen is slightly different. The result is depicted with other curves in Fig. 5. The minimum lies around 50 m/min, and the curve levels off above the speed of 100 m/min. Damping forces from the cutting process increase below 50 m/min, and the stability limit rises sharply. The curve was also measured for higher cutting speeds than the curves supplied by other laboratories. The conditions for orthogonal turning of steel AISI 1045 were the same in all experiments. The results should therefore be comparable.

Tlusty, Moriwaki and Goel [Goel 1976] published stability graphs for several carbon steels in 1976. The tests were run under the standard conditions of the previous collaborative CIRP project. The graphs were calculated on the basis of DCFC measurements for a typical mechanical vibrating machine tool system. They are not stability limits obtained from machining tests. The curves shown are, nevertheless, indirectly related to machining during measuring DCFC. The authors observed the influence of feed and wear on DCFC and showed the effect of these in the graphs of the depth of cut in turning (Fig. 4).

The first four graphs from the legend to Fig. 4 have the same flank wear VB=0.05 mm. This is approximately the boundary between a slightly worn and a sharp tool. It can be seen from the vertical position of the curves that stability improves with increasing feed and flank wear. The characteristic of the curves is basically the same. The fall in stability has its minimum approximately in the speed range of 90 to 120 m/min. If the flank wear increases from 0.05 to 0.20 mm, i.e. four times, the character of the curve does not change, but the limit grows slightly. The curve for steel 4340, (alloy steel with 36NiCrMo4) has a completely different characteristic than previous curves. VB is increased to 0.15 mm. The measured points fluctuate considerably. It remains to be seen to what extent it will be possible with this material to keep the tool wear constant during the whole test.

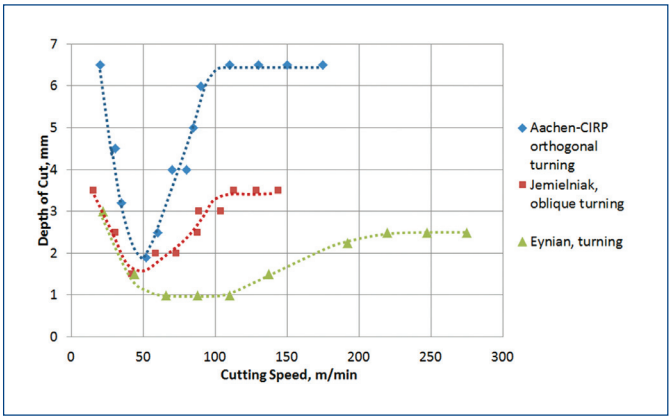

Figure 5. *Stability curves. Data compiled after [Peters 1972], [Jemielniak 1992] and [Eynian 2010b].*

Jemielniak [Jemielniak 1992] investigated possibilities of determining dynamic cutting force coefficients by measuring static forces in turning. In his model he defined specific stiffness coefficients and specific damping coefficients. The model was verified using a machining test. The result of the test is shown in Fig. 5 and again clearly indicates a drop in stability with a minimum around 40 to 50 m/min. The shape of the curve is similar to the Aachen measurement including the position of the stability limit minimum. Similar results for turning stability were published by Eynian [Eynian 2010b] in his doctoral thesis from 2010 (see also Fig. 5). It was a case of 3D longitudinal turning with an approach angle Kappa of 95°. The workpiece was made of steel AISI 1045, had a diameter of 41.3 mm and L= 235 mm, and was chucked.

Altintas, Eynian and Onozuka [Altintas 2008] also published a cutting test, performed earlier than the previous one, the result of which was different. The drop in the stability limit did not occur. A workpiece made

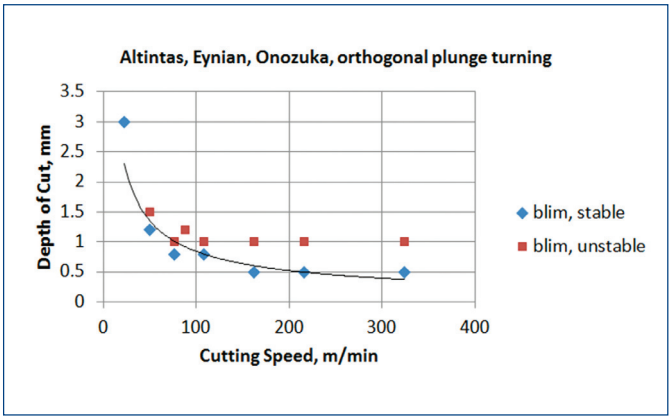

Figure 6. *Plunge orthogonal turning, steel AISI 1045. Grooving tool with a 2.4 mm edge width, 7° rake, and 7° clearance angles. Data after [Altintas 2008].*

of steel AISI 1045 with a diameter of 35 mm was machined using an orthogonal plunge turning operation (see Fig. 6). The test is also described in [Eynian 2010b]. Similar stability curves in the shape of letter L are described by Sisson and Kegg in [Sisson 1969]. However, they do not state any clearance angle.

Liu C. R. and Liu T. M. [Liu 1985] examined the possibilities of chatter suppression by modifying tool geometry. They face-turned a steel thick-walled tube orthogonally. By tilting the tool holder in a special tool head, they changed both the rake and clearance angle. They produced the results depicted in Fig. 7.

With rake angles (RK) of -5°, 0°, and 5° and clearance angles (CL) of 16°, 11° and 6°, the stability curves have the shape of the letter L. The change of clearance angle from 6° to 1° caused a change in the shape of the stability curve to a bowl shape. Curves have practically the same characteristic for the lowest cutting speeds. However, the stability measured for CL=1° rises sharply above the speed of 80 m/min, whereas the curves for CL=6°, 11° and 16° rise only slightly. The change in the rake angle from –1° to 10° did not change the bowl shape of the stability curve. It only shifted the curve.

It is interesting to compare these results with the results published by W. A. Knight in [Knight 1972]. Knight used tools with rake angles 5°, 15° and 25° and clearance angle 5°. He investigated the influence of the rake angles on stability. In all the three cases, he found that stability declines with a drop in work speed to the minimum. Moreover, these tests confirmed that stability rises with higher speeds, and the bowl-shaped curves level off.

3. Examples of milling test results

Sisson and Kegg in [Sisson 1969] present an example of aluminium end milling. Eynian and Altintas [Eynian 2010a] milled steel AISI 1045 with a hardness of 21 HRC, using a two-tooth milling cutter with D=18 mm and a carbide insert. The chatter frequency was 767 Hz at n=3581 rpm and a_e=D=18 mm. As the results were very sensitive to tool wear, the tool wear was kept at 130 μm. For the results of the researchers refer to Fig. 9. The stability limit increases monotonously with a decrease in cutting speed. Bach in [Bach 2008] presents the result of measuring the stability limit for milling titanium alloy Ti6Al4V (see Fig. 10). The four-tooth PM-HSS tool with a diameter of 32 mm, length of active part 106 mm, and a_e=1 mm was used for milling. Tools had both regular and irregular tooth pitch.

4. New tests

In order to investigate the influence of technological parameters on the shape of curves, an experiment was carried out (see Fig. 11). A stiff workpiece was chucked and a cutting tool machined the workpiece with a radial motion perpendicular to the tool holder shank. Test conditions are shown in Tab. 1. Revolutions were kept at a constant value of 700 rpm and 900 rpm resp. so that the cutting speed decreased continuously during machining. The tool holder for boring holes was slim and had a diameter of 12 mm and L/D=5.4 for the 1st and 2nd trial and a diameter of 20 mm and L/D=6.25 for the 3rd and the 4th trial so that it vibrated easily and created a vibrating system. The stability limit was measured for both possible directions of motion: from the centre of the workpiece to its circumference as well as in the opposite direction (+x and -x axis), Fig. 12). Machining was oblique with a minimum force in the direction of the z axis.

The shape of both the measured curves is close to curves for milling, especially curve R08 (nose radius R=0.8 mm), which has the shape of a hyperbole (see Fig. 12). The curve denoted as R02 resembles the letter L. The change in the curve shape was only caused by replacing

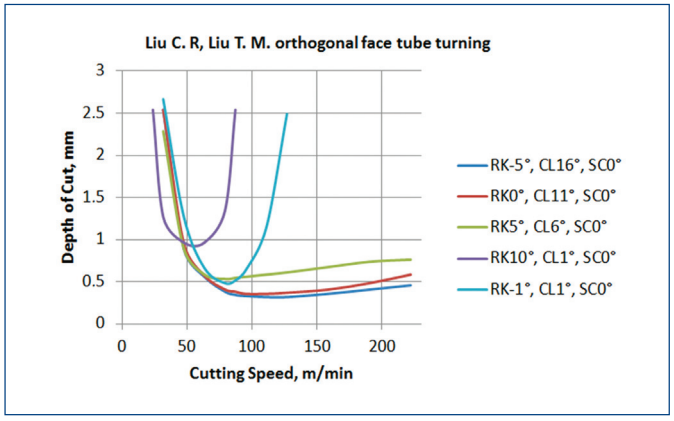

Figure 7. *Orthogonal face turning of a thick-walled tube. Data compiled after [Liu 1985].*

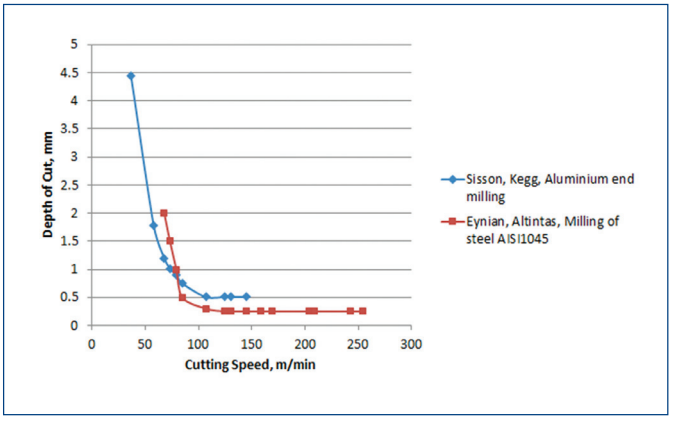

Figure 9. *Stability of aluminium and steel milling. Compiled after [Sisson 1969] and [Eynian 2010a].*

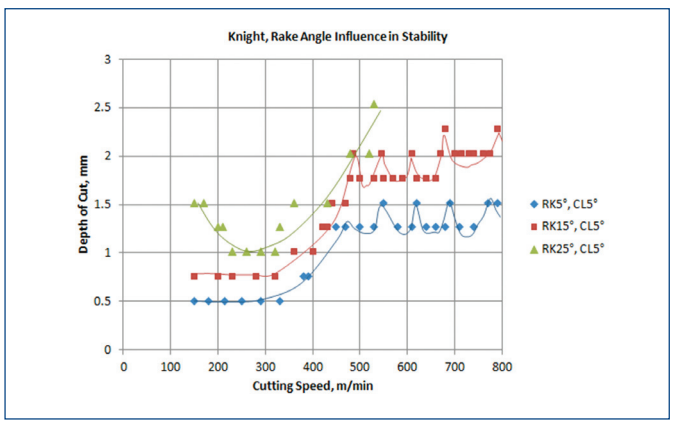

Figure 8. *Rake angle effect in lower speed stability. Feed rate 0.129 mm/rev. Compiled after [Knight 1972].*

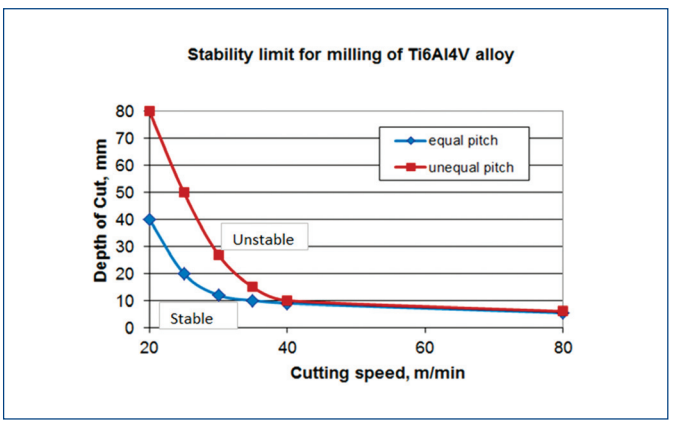

Figure 10. *Stability limit for milling titanium alloy Ti6Al4V. A PM-HSS tool with Ø D32 mm, a_e=1 mm, and f_t=0.05 mm. After [Bach 2008].*

	Material of sample	Insert type	RK [°]	CL [°]	AP [°]	Feed rate [mm/rev]	Cutting speed range [m/min]	Tool wear [mm]	Operation type
1st trial	AISI 1045	CPMT 080808 NSU	8	11	95	0.1	41 – 163	0.03 – 0.157	Oblique face turning
2nd trial		CPGT 080202 NSU	8	11			58 – 220		
3rd trial		CNMG 090308 NGU	7	0			40 – 220		
4th trial		CNMG 090308 NSU	13	0			60 – 280		

Table 1. *Cutting conditions for the new tests*

the insert with a nose radius of 0.8 mm (for light/medium cut) by an insert with a nose radius of 0.2 mm (for finishing cut). The tool holder during the 1st and 2nd trial remained the same, as did the machine configuration and the workpiece setup.

Although both the curves show an increase in the stability limit with falling cutting speed, the stability limit of the tool with the R02 radius increases very sharply in comparison with the increase of the curve for R08. Judging from curve R02 it seems that stability starts to rise sharply from the point DOC=0.2 mm, where the depth of cut exceeds the size of the insert nose radius. The stability limit is several times higher at higher speeds than for R08. The second curve, valid for R08, also shows a significant increase in DOC, while the radius R=0.8 mm was in all points larger than the depth of cut. We assume from a comparison of both curves that at lower speeds (here below 70 m/min), a sharp tool tip may not be able to dampen chatter vibrations so well as the bigger radius R08. Machining with a R02 insert is similar to orthogonal machining because the force in the direction of the rotary axis is very small. The result of the 3rd and 4th trial is depicted in Fig. 13. In this case the only significant change of the cutting conditions was the decrease in the clearance angle. Clearly, it caused the change in the stability limit curves from L-shaped curves to U-shaped curve for RK=13°or bowl-shaped curves for RK=7°.

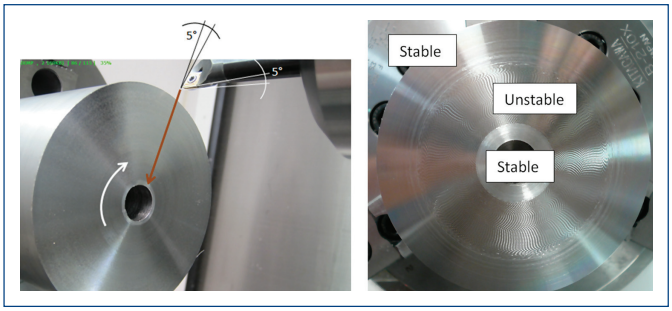

Figure 11. *Left: Illustration of the test setup. Face-end turning from the circumference to the centre of the workpiece. Right: Example of machined surface.*

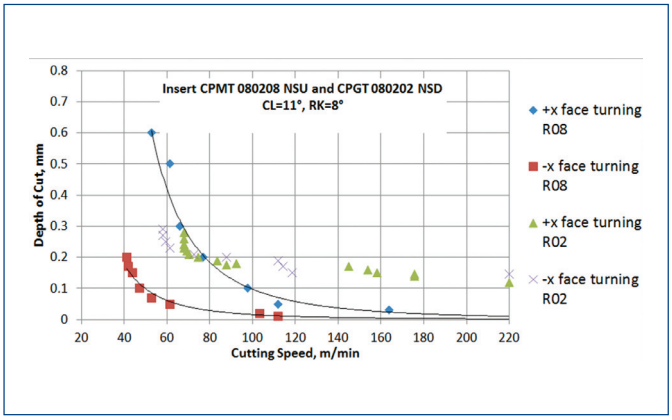

Figure 12. *Light and finish plunge/face turning stability with clearance angle CL=11°. Influence of the tool nose radius and clearance angle.*

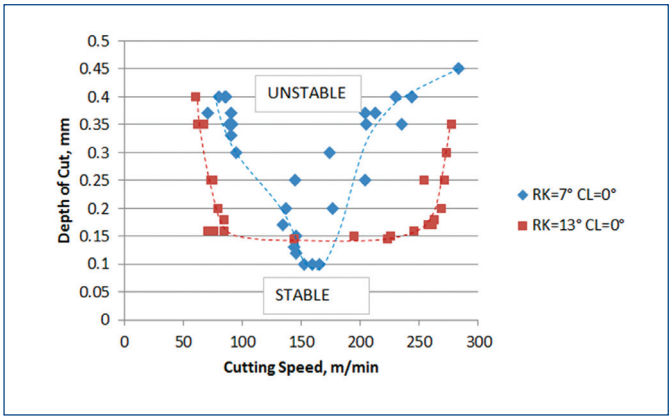

Figure 13. *Light and finish plunge/face turning stability with clearance angle CL=0°. Influence of the rake angle on the unstable field.*

5. Comparison of the cutting test condition

Conditions under which the stability limit curves above were measured are presented in Tab. 1 (new tests), Tab. 2 (earlier turning tests) and Tab. 3 (earlier milling tests). Unfortunately, the data gathered in the tables are neither complete, nor entirely consistent. Test conditions differ to some extent. It is not always possible to keep the conditions in tests constant. Therefore, the conclusions drawn below are only valid with a certain degree of probability.

The following can be said about stability curves based on the measured stability limit curves and Tab. 1, Tab. 2 and Tab. 3.

a) Shape L and U of a stability curve is influenced the most by the clearance angle. Shape U, i.e. the drop in the stability limit in a certain range of low cutting speeds, will only appear with small clearance angles, probably with angles smaller than 5° – 7°. Fig. 13. Light and finish plunge/face turning stability with clearance angle CL=0°. Influence of the rake angle on the unstable field.

b) If the clearance angle is small, the occurrence of the U-shaped curve is more probable than in orthogonal turning or in operations similar to it, with small insert radii.

c) A larger nose radius does not change the shape of either the L or U curve. It changes the curvature of the L curve. The level of stability is higher in the +x axis (see Fig. 12. Light and finish plunge/face turning stability with clearance angle CL=11°. Influence of the tool nose radius and clearance angle.). It could be a consequence of a smaller effective clearance angle.

d) The rake angle reduces the stable field because it enlarges the bowl-shaped curve to the U curve, as shown in Fig. 13. Light and finish plunge/face turning stability with clearance angle CL=0°. Influence of the rake angle on the unstable field. After that of Liu C R and Liu T M [Liu 1985], it only shifts the U curve both horizontally and vertically.

e) If the insert (particularly the flank and the nose) is slightly worn, it does not interfere with the continuity of curves, nor does it change their shape in any considerable way. Sudden wear (minor destruction of the insert nose) results in an accidental error of the measured point (see e.g. Fig. 12. Light and finish plunge/face turning stability with clearance angle CL=11°.

Authors	Rake angle [grad]	Clearance angle [grad]	Aproach/side angle [grad]	Flank wear VB [mm]	Workpiece L/D [mm]	Operation type	Stability curve shape
Sisson, Kegg [1]	not stated	5	not stated	not stated	not stated	orthogonal turning	U curve
Kals [2]	5	6	90	not stated	not stated	orthogonal turning	U curve
Peters et al, CRIP [3]	3	7	not stated	less than 0.1	clamped in chuck and tailstock centre	orthogonal turning	U curve
Aachen, CRIP [3]	3	7	not stated	less than 0.2			
Tlusty, Moriwaki, Goel [4]	3	7	not stated	varied from 0.05 and 0.2			
Jemielniak [5]	not stated	11	80	max 0.05	not stated	olique turning	U curve
Eynian [6]	not stated	not stated	95	0.075 fresh 0.175 worn	chucked 235/41.3	olique turning	U curve
Altintas, Eynian, Onozuka [7]	0	7	95	sharp/worn tool	chucked	orthogonal **plunge** turning	L curve
Liu C. R., Liu T. M. [12]	–1	1	90	not stated	tube, D = 101 mm wall thickness 4.8 mm	orthogonal face turning of a **tube**	U curve
		11					L curve
	varied (–5:10)	varied (16:1)					U/L curve

Table 2. *Earlier studies – an overview of cutting (turning) tests conditions.*

Authors	Material of sample	Clearance angle [grad]	A_e [mm]	Feed rate [mm/flute]	Cutting speed range [m/min]	Tool wear VB [mm]	Dool D/ teeth [mm]	Chatter frequency [Hz]	Operation
Sisson and Kegg [1]	aluminium	5	not stated	not stated	40 – 140	not stated	13/?	tool L/D = 60/12, 4300	end milling
Eynian and Altintas [8]	steel AISI 1045	R390-11 T302E-PM4240 insert	slotting	0.1	70 – 260	0.13	18/2	767	
Bach [9]	Ti6Al4V	6	1	0.1	20 – 80	0.2	32/4	not meas.	
Bach [10]	steel	not stated	slotting	0.05	37 – 67	not measured	32/4	747	

Table 3. *Data for milling operations, earlier studies.*

Influence of the tool nose radius and clearance angle. v_c=100 – 120 m/min).

f) Other aspects such as workpiece material, operation type, approach angle, feed rate, cutting speed range and workpiece clamping do not influence the stability curve shape significantly. A different work clamping can change the vibrating system stiffness.

g) All milling tests resulted in a stability curve in the L shape, i.e. without the drop in stability.

Concluding this part of investigation, we can say that the main parameters which effect stability at lower cutting speed are clearance angle, rake angle and insert nose radius.

6. Causes of the stability limit drop in turning

Tlusty analyses the results of the collaborative research on measuring dynamic cutting force coefficients for turning, and presents, among other things, the dependence of DCFC on cutting speed [Tlusty 1978]. We will adopt the data and notation of the equations in order to analyse causes of the stability drop in the turning operations at lower cutting speeds. The equations for two components of a single cutting force were assumed:

$$\begin{aligned} F_N &= b\left(-K_{di}Y_i + K_{do}Y_o\right) = -F_{di} + F_{do} \\ F_T &= b\left(-K_{ci}Y_i + K_{co}Y_o\right) = -F_{ci} + F_{co}, \end{aligned} \tag{1}$$

where F_N (thrust force) is the component "normal" to the cut surface and it has the direction of Y (tool vibration). F_T (main cutting force) is the component "tangential" to the cut surface. The subscripts d and c denote the "direct" and "cross" effect of vibration in direction Y respectively. The subscripts i and o denote "inner" and "outer" modulation. The letter b is an equivalent to the nominal width of cut. Y_i denotes tool vibration, Y_o denotes waves left on the cut surface during a previous cut. At the limit of stability it is:

$$|Y_o| = |Y_i|, Y_o = Y_i e^{j\varepsilon}. \tag{2}$$

The forces F_{di}, F_{ci} and F_{do}, F_{co} are the components modulated by tool vibration and work undulated surface respectively. The dynamic cutting force coefficients K_{di}, K_{do}, K_{ci}, K_{co} were assumed complex. The equations (1) can be expressed in goniometric form (3) and depicted in the complex plane, see Fig. 14 and Fig. 15.

$$\begin{aligned} F_N &= b\cdot|K_{do}|\cdot Y_i\cdot e^{j(\psi_{do}+\varepsilon)} - b\cdot|K_{di}|\cdot Y_i\cdot e^{j\psi_{di}} = |F_{do}|\cdot e^{j(\psi_{do}+\varepsilon)} - |F_{di}|\cdot e^{j\psi_{di}} \\ F_T &= b\cdot|K_{co}|\cdot Y_i\cdot e^{j(\psi_{co}+\varepsilon)} - b\cdot|K_{ci}|\cdot Y_i\cdot e^{j\psi_{ci}} = |F_{co}|\cdot e^{j(\psi_{co}+\varepsilon)} - |F_{ci}|\cdot e^{j\psi_{ci}} \end{aligned} \tag{3}$$

For stability limit can be after [Tlusty 1978] written:

$$b_{\lim} = \frac{2k\left(1-p^2+2j\xi p\right)}{\left(-K_{di}-K_{ci}\right)+\left(K_{do}+K_{co}\right)\cdot e^{j\varepsilon}}, \tag{4}$$

where k and ξ denote stiffness and damping ratio respectively of a single degree of freedom system. The letter p indicates a frequency ratio. Real parts of coefficients K_{do} and K_{co} in Eq. (1) can be replaced by real parts of coefficients K_{di} a K_{ci}, whose dependences on cutting speed are in fact the same, as presented in that of Goel [Goel 1976]. Under certain conditions specified in that of [Tlusty 1978], it is possible to deduce the simplified relation for the stability limit:

$$b_{\lim} = \frac{4k\xi}{\{\mathrm{Re}(K_{di})+\mathrm{Re}(K_{ci})-\mathrm{Im}(K_{di})-\mathrm{Im}(K_{ci})\}}. \tag{5}$$

The components Re(K), and Im(K) resp. are real and imaginary parts of DCFC. Dependences of measured coefficient components of inner modulation on cutting speed, as presented by Tlusty [Tlusty 1978], are shown in Fig. 16. Using these data, and for certain selected

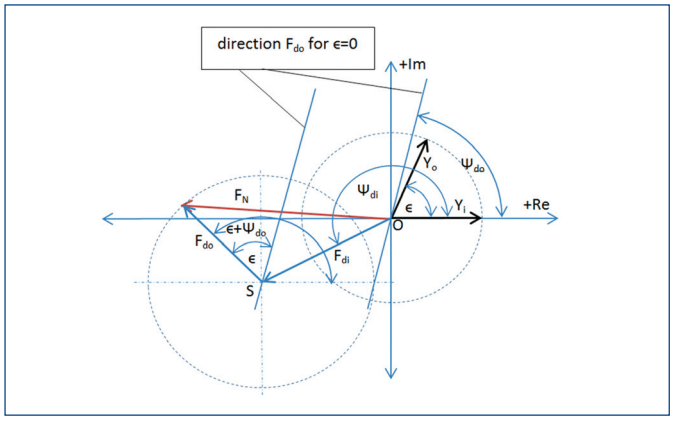

Figure 14. *Equation for the thrust force F_N depicted in the complex plane*

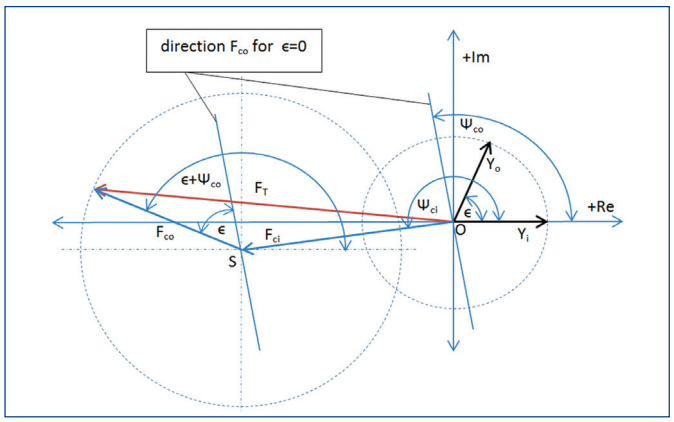

Figure 15. *Equation for the tangential force F_T depicted in the complex plane*

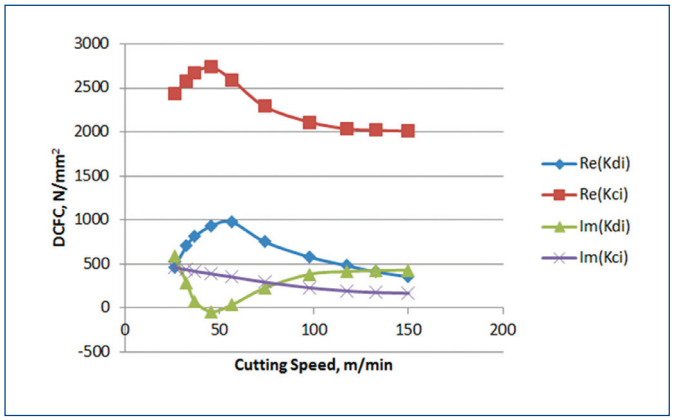

Figure 16. *Real and imaginary components of dynamic cutting force coefficients for turning. Data compiled from [Tlusty 1978] and [Peters 1972] and averaged. Material: steel 1045.*

values k and ξ (these values do not influence the curve shape), we are able to calculate the dependence of the stability limit on cutting speed in Fig. 17, which is the bowl-shaped curve.

If we consider the just-described changes in real and imaginary components of complex coefficients in the accepted cutting force model (1), we discover that phases of the force F_{di} in relation to tool chatter Y_i change with cutting speed according to the curve shown in Fig. 18. The phase of the tangential force F_{ci} changes very little.

Slightly more consistent data for DCFC can be found in [Rao 1977]. Calculating the phases of the components F_{di}, F_{do}, F_{ci}, F_{co}, we can recognize the deep drop in the phases (even under the zero

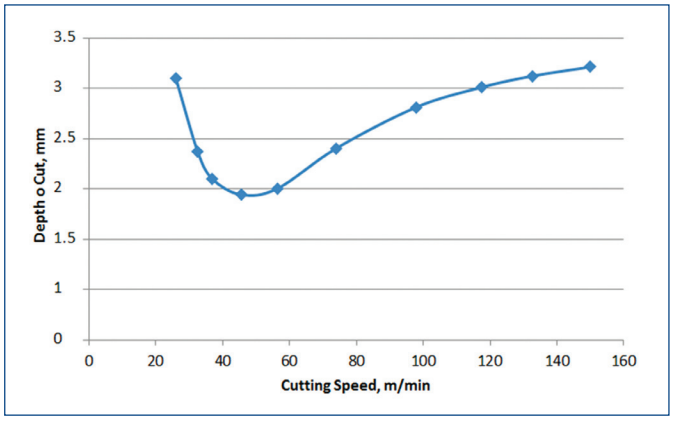

Figure 17. *Limit of stability for turning calculated with the use of data published in [Tlusty 1978] and [Peters 1972].*

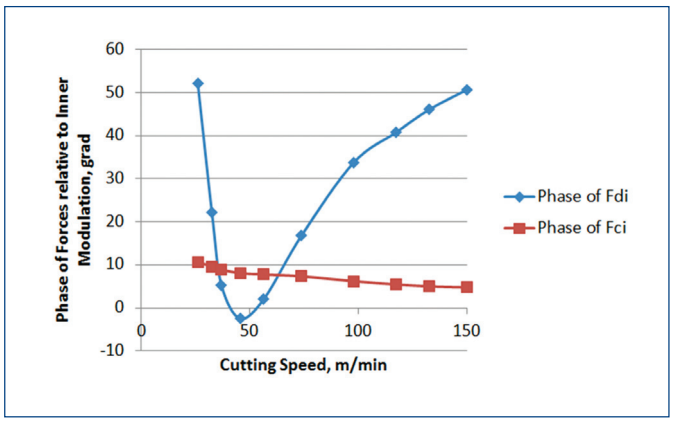

Figure 18. *A change in phases of the direct and tangential force components F_{di} and F_{ci}. Compiled after [Tlusty 1978]. Material: Steel 1045.*

value) in between speeds 50 and 100 m/min, which is a close speed range to the previous example. Moreover, the component F_{di} of the thrust force and the component F_{ci} of the tangential force exhibit a mutual phase. The same is true of the forces F_{do} and F_{co}.

The third example presented here compiled data after that of Goel [Goel 1976], Fig. 20. In this case only F_{di} exhibits a significant phase shift change against Y_i with a minimum at 60 m/min. Again the cutting force components F_{di} and F_{ci} and also F_{do} and F_{co} are phase shifted. The accented phase shift of the components means that the resulted thrust and tangential forces F_N, F_T are also phase shifted. This fact indicates independence of the two forces and moreover an existence of some further forces acting in the unstable cut.

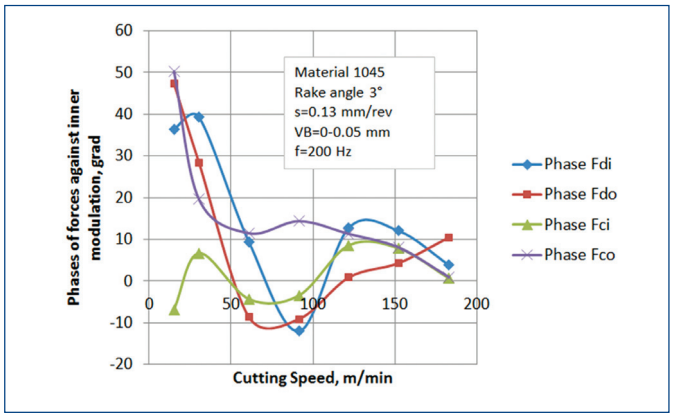

Figure 19. *Phases of the components of the thrust and main cutting force. Compiled after [Rao 1977].*

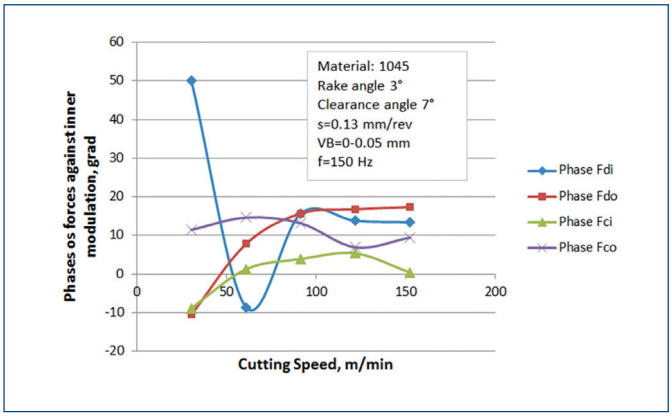

Figure 20. *Phases of the components of the thrust and main cutting force. Compiled after [Goel 1976].*

7. Conclusions

a) A comparison of the conditions used in the tests by turning shows that the decline in the limits of stability and its subsequent increase in the area of low cutting speed occurs only when using the tool with a small clearance angle. This corroborates the commonly accepted theory of tool contact with the wavy machined surface. It seems to be evident that the drop in the stability curve appears while turning with an insert which has a clearance angle less than 5° – 7°. The rake angle does not cause stability decline, but it affects the width of the stable range as well as the position of the U-curve within the b_{lim}-v coordinates. (See Fig. 7, Fig. 8 and Fig. 13). There is no evidence of a stability drop when milling.

b) The stability drop is strongly influenced by the phase of cutting forces against tool vibration Y_i, see Fig. 18, Fig. 19 and Fig. 20.

c) The cutting force components F_N and F_T are phase shifted mutually. (See Fig. 14 and Fig. 15). Hence, these two forces are independent forces, not components of a single cutting force. Very probably, the mutual shift is influenced by the existence of some additional forces acting in the unstable cut.

8. Future work

The reason why the forces change the phase against Y_i, is a challenge for future research. Some preliminary studies point to processes in the area of the shear plane. The study of processes in the area of the tool flank is also important, especially when we are aware of the influence of the clearance angle on the shape of the stability curves. We feel there is a necessity for a detailed study, which would identify the independent dynamic forces acting in the cut when turning.

Acknowledgements

Thanks are due to the company Misan s.r.o., Lysa nad Labem, Czech Republic for providing the tools and machine for cutting tests. The research has been funded within the framework of the grant TE01020075 Competence Centre – Manufacturing Technology of the Technology Agency of the Czech Republic.

References

[Altintas 2008] Altintas, Y., Eynian M., Onozuka H. Identification of Dynamic Cutting Force Coefficients and Chatter Stability with Process Damping, CIRP Annals MT, 2008, 57, 1, 371-374.

[Bach 2008] Bach P. HSS Tools made of PM Steels used for Titanium Alloys Milling, A lecture at The Czech Toolmakers Conference during, the exhibition For Industry, Prague, (in Czech), 2008.

[Bach 2011] Bach P., Svoboda O. Influence of Technology on Milling Spindles Stability, A lecture at Customers Days of Misan, s. r. o., Lysa nad Labem, (in Czech), 2011.

[Eynian 2010a] Eynian M., Altintas Y. Analytical Chatter Stability of Milling with Rotating Cutter Dynamics at Process Damping Speeds, Journal of Manufacturing Science and Engineering, April 2010, 132, 2.

[Eynian 2010b] Eynian M. Chatter Stability of Turning and Milling with Process Damping, Vancouver: A Thesis for the Degree of Ph. D., University of British Columbia, 2010.

[Goel 1976] Goel B. S. Measurement of Dynamic Cutting Force Coefficients. Hamilton: McMaster University, 1976.

[Jemielniak 1992] Jemielniak K. Modeling of Dynamic Cutting Coefficients in Three-Dimensional Cutting, Int. J. Mach. Tools Manufacturing, August 1992, 32, 4, 509-519.

[Kals 1971] Kals H. J. J. On the Calculation of Stability Charts on the Basis of the Damping and Stiffness of the Cutting Process, CIRP Annals, 1971, 19, 297.

[Knight 1972] Knight W. A. Chatter in Turning: Some Effects of Tool Geometry and Cutting Conditions, Int. J. Machine Tool Design and Research, 1972, 12, 3, 201–220.

[Liu 1985] Liu C. R., Liu T. M. Automated Chatter Suppression by Tool Geometry Control, Journal of Engineering for Industry, 1985, 107, 2, 95-100.

[Peters 1972] Peters J., Vanherck P., van Brussel H. The Measurement of the Dynamic Cutting Coefficient, CIRP Annals, 1972, 21, 2.

[Rao 1977] Rao S. B. Analysis of Dynamic Cutting Force Coefficient, Hamilton: McMaster University, 1977.

[Sisson 1969] Sisson T. R., Kegg R., L. An Explanation of Low Speed Chatter Effects, Journal of Engineering for Industry, November 1969, 91, 4, 951-958.

[Tlusty 1963] Tlusty J., Polacek M. The Stability of the Machine-Tool against Self-Excited Vibration in Machining, the IRPE Conference, ASME, Pittsburgh, 1963.

[Tlusty 1976] Tlusty J., Moriwaki T., Goel B. S. The Dynamic Cutting Coefficient for Some Carbon Steels, Proc. 4th NAMR Conf., Battelle's Labs, Columbus, 1976.

[Tlusty 1978] Tlusty J. Analysis of the Research in Cutting Dynamics, Annals of the CIRP, 1978, 27, 2, 583-589.

Contacts

doc. Ing. Pavel Bach, CSc., Ing. Milos Polacek, CSc.
Ing. Petr Chvojka, Ph.D., Ing. Jiri Drobilek
Czech Technical University in Prague
Faculty of Mechanical Engineering
Department of Production Machnies and Equipment
Research Center of Manufacturing Technology
Horska 3, Prague 2, 128 00, Czech Republic
tel.: +420 221 990 935, fax: +420 224 359 348
e-mail: info@rcmt.cvut.cz, www.rcmt.cvut.cz

Ing. Ondrej Svoboda, Ph.D.
Misan, s. r. o
Ke Vrutici 1795, Lysa nad Labem, 289 22, Czech Republic
tel.: +420 551 440, e-mail: lysa@misan.cz, www.misan.cz